ISSN PRINT 2319 1775 ONLINE 2320 7876

 Journal Volume 10 , Iss 2, Feb 2021

Improved Power Quality Transformerless Single-Stage Bridgeless Converter Based Charger for Light Electric Vehicles

Dr. V. S. Dhok[1], Mr. P. V. Ambade[2], Prof A.V. Joshi[3], Mr. Vikas Raghorte[4]

[1]Associate Professor, Department of EEE, J D College of Engineering & Management, Nagpur
[2,3]Assistant Professor, Department of EEE, J D College of Engineering & Management, Nagpur
[4]Student, Department of EEE, J D College of Engineering & Management, Nagpur

ABSTRACT:
In this article, a bridgeless switched inductor Cuk (BSIC) converter based charger is presented to provide the low-cost and reduced-size charging solution for the light electric vehicles, i.e., LEVs, with enhanced performances at the supply side. Generally, the chargers of LEVs such as E-Rickshaws, E-Bike, and E-Cycle, are equipped with an additional converter to charge the batteries at low voltages (24–72 V). The switched inductor configuration improves the step-down dc voltage gain of the charger with only one stage and also improves the reliability at such low voltages. It is noteworthy that the cost associated with the sensors along with the size of the magnetic components is considerably reduced by operating the charger in discontinuous current mode condition. Moreover, the high-gain transformerless configuration further improves the cost, size, and efficiency of the charger. The effectiveness of the charger is tested on a laboratory prototype, for an 850 W rating with 220 V, 50 Hz nominal supply voltage conditions. The steady state and dynamic behaviors of the charger are analyzed under different operating conditions. Moreover, the behaviors of the charger during the initialization of charging process are analyzed for ensuring the soft starting of the charger. A basic comparison of the presented charger configuration with existing LEVs chargers is presented to highlight its advantages over the existing one.

1. INTRODUCTION

Since the percentage demand of the LEVs is increasing manifolds, the charging facility equipped with an improved power quality solution is much anticipated from the power distributors as well as the consumer's perspectives [1]. The existing chargers for the LEVs generally consist of an isolated/nonisolated dc–dc converter, followed by a combination of diode bridge rectifier (DBR) and dc link capacitor (CDC), as shown in Fig. 1. The combination of DBR with a heavy dc-link capacitor draws harmonics-rich distorted current from the supply, and therefore, it deteriorates the input power factor (PF), distortion factor (DF), displacement factor (DIF), and efficiency of Manuscript received March 31, 2020; revised October 6, 2020; accepted December 18, 2020. Date of publication January 1, 2021; date of current version March 5, 2021. This work was supported in part by the J C Bose Fellowship under Grant RP03128 and in part by the FIST Scheme under Grant RP03195G. Recommended for publication by Associate Editor M. Peretz. (Corresponding author: Jitendra Gupta.) The authors are with the Department of Electrical Engineering, IIT Delhi, New Delhi 110016, India (e-mail: jitendra.gupta2210@gmail.com; radhakushawaha@gmail.com; bsingh@ee.iitd.ac.in). Digital Object Identifier 10.1109/TPEL.2020.3048790

Research paper **© 2012 IJFANS. All Rights Reserved, Journal Volume 10 , Iss 2, Feb 2021**

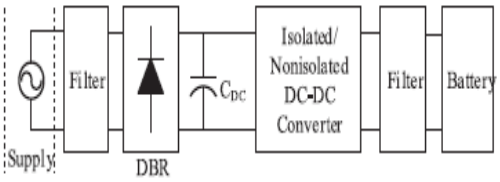

Fig. 1. Structure of conventional charger configurations for LEVs.

the charger [2]. The single-phase active power factor correction (APFC) methods are extensively utilized to eliminate the abovementioned drawbacks of the conventional low power rating chargers. In an APFC method, a dc–dc converter is employed between DBR and CDC, to improve the supply-side performances of the charger from a power quality point of view. It is noteworthy that an APFC converter can perform multiple tasks in a charger based on the configuration of a charger, i.e., single-stage chargers or double-stage chargers. In a double-stage configuration, an APFC is employed to fulfill supply-side requirements and another dc–dc converter is required for satisfying the load-side demands, whereas only an APFC dc–dc converter performs both the tasks in the single-stage chargers. Several two-stage charger configurations based on different APFC solutions have been explored for the EVs/LEVs charging applications [3]–[5]. However, each solution has its benefits and drawbacks regarding its device count [6], conduction and switching losses [7], control complexities [5], and efficiency [8]. In order to improve the charger's efficiency by reducing its conduction losses in the APFC stage, many bridgeless APFC converters with partial [9] or complete [10] elimination of the DBR have been reported in the literature. A detailed review of bridgeless APFC converters is given in [11]. Recently, some bridgeless integrated charging solutions have been suggested to improve the component count and losses in the chargers while retaining the advantages of the two-stage chargers [12], [13]. In an integrated configuration, the semiconductor devices have been shared by both dc–dc converters, which reduce the device count and associate losses. However, the increased control complexities and high device stresses make them less attractive for LEVs applications. The ripple-free charging current is considered as a major advantage of a single-phase two-stage charger. However, several authors have claimed that low-frequency ripples in the charging current, if controlled properly, do not affect performance of the battery [14], [15].

While addressing these drawbacks of two-stage chargers, several researchers have provided various single-stage charger configurations for the EVs/LEVs along with enhanced power quality at the supply side [16], [17]. The single-stage chargers have high power density [18], less component count [19], and a simplified control structure [20]. Moreover, a properly designed single-stage charger configuration can provide better efficiency than its two-stage counterpart. The limited output voltage capability of the conventional boost converter and the high distortion in the supply current near the zero crossing in the conventional buck converter [21] rule out the possibilities of their application as an APFC in the single-stage LEVs chargers. Therefore, in most of the cases, the shortcomings of buck and boost derived converters are eliminated by employing the buck–boost derived converters such as buck–boost, Cuk, SEPIC, Zeta, CSC, and Luo dc—dc converters. The Cuk dc–dc converter shows excellent input and output current ripple characteristics among all buck–boost dc–dc converters [22]. However, the conventional buck–boost dc–dc converters are less suitable to provide a transformerless single-stage charging solution for the LEVs, due to their limited gain capability. In the case of LEVs, due to low battery voltage, the transformerless charger configuration operates at a very low duty ratio, which ultimately affects the charger's

Research paper **© 2012 IJFANS. All Rights Reserved, Journal Volume 10 , Iss 2, Feb 2021**

dynamic performance and efficiency [23]. Therefore, most of the single-stage LEVs chargers based on conventional dc–dc converters require a transformer for getting the desired dc voltage gain. However, the inclusion of the transformer increases the cost and size of the charger. Moreover, the leakage inductance of the transformer increases the voltage stress across the devices [24]. Consequently, the development of the single-stage transformerless charger for the EVs is gaining the researcher's attention nowadays [25]. However, the improved power quality based transformerless charger configuration for the LEVs is still rarely addressed by the researchers. Several efforts have been made recently to improve the voltage gain capability of conventional dc–dc converters such as by utilizing coupled inductors, by cascading of converters, by employing quadratic converters, by considering multiplier circuit, interleaved front end structure, and switched inductor or hybrid switched inductor–capacitor structure [26]. In the case of coupled inductors, operating characteristics of the converter largely depend upon the coupling coefficient whereas the cascading and multiplier approach in converters increases the component count, which leads to higher cost, low efficiency, and complex circuitry. However, the quadratic converter provides higher efficiency than cascaded converter at the cost of increased voltage and current stresses [27]. In order to overcome these issues, a switching dual network based on split capacitors or split inductors along with two to three diodes is proposed in [28]. The switched inductor (SI) and switched capacitor (SC) networks efficiently modify the dc gain of conventional converters, based on the series/parallel charging and parallel/series discharging of the capacitors or inductors. In [29], an SI Cuk PFC converter based charger is proposed for LEVs. However, this charger has a high cost, complex control, and has increased size of magnetic components due to CCM

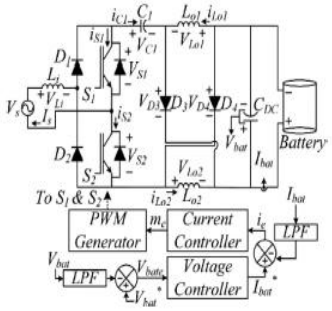

Fig. 2. BSIC PFC converter based transformerless charger configuration.

operation. Moreover, the DBR at the front side increases the conduction losses and component count in the charger.An enhanced power quality charger based on a single-stage configuration of BSIC PFC converter is presented in this work.

Main contributions of this article are highlighted as follows.

1) This charger provides a single-stage charging solutionfor the LEVs, without having a transformer or coupled inductors with minimum component counts.

2) The design and control of the BSIC converter are carried out under the DCM condition, which not only reduces the size of magnetic components and associated losses but it also reduces the sensor requirements. Furthermore, the DCM operation rules out the need for the PLL system, and therefore, it considerably simplifies the control implementation part.

3) The bridgeless structure at the front side reduces total device counts and the conduction losses of the charger.

4) Additionally, the enhanced power quality operation of the charger is tested and verified over a wide range of supply voltage while implementing the constant-current and constant-voltage charging modes.
5) A comparative analysis of the presented charger configuration with a conventional Cuk PFC converter [4] and an SI Cuk PFC converter [29] is carried out and presented based on various factors, e.g., number of components, control complexities, cost, size, and supply-side performances.

2. BATTERY CHARGER CONFIGURATION

The single-phase single-stage charger configuration based on the BSIC PFC converter is depicted in Fig. 2.

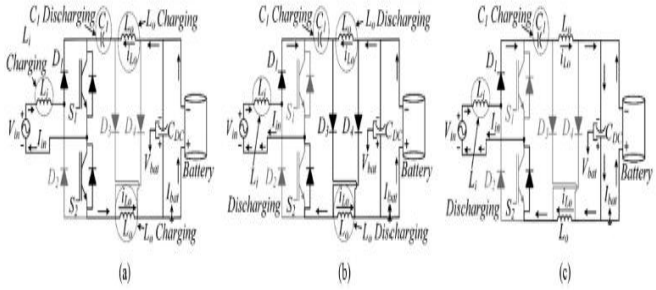

Fig. 3. Operating modes of bridgeless switched inductor Cuk PFC converter in a switching cycle (positive half-cycle). (a) Mode-P(I) (t_0-t_1). (b) Mode-P(II) (t_1-t_2). (c) Mode-P(III) (t_2-t_3).

This configuration implements a single-phase single-stage transformerless ac–dc converter for the LEVs charging application with additional high step-down gain capabilities and improved power quality performances at the supply side. The bridgeless structure at the front side is supplied by a single-phase supply with a nominal voltage (Vs) rating of 220 V, 50 Hz. The input inductor (Li) serves the purpose of the Cuk converter input inductor as well as it acts as a filter for the supply current (Is). The forward leg of the front-end bridge constitutes of two diodes D1 and D2, while the second leg consists of two active switches S1 and S2, unlike the conventional DBR, which has the combination of four diodes. D1 and D2 operate for the positive and negative half-cycles of supply voltage, respectively, whereas both switches (S1 and S2) are switched simultaneously irrespective of supply voltage polarity to reduce the control complexities. The intermediate capacitor (C1) serves a similar purpose as the conventional Cuk PFC converter. At the load side, an SI network is provided, which consists of a combination of two inductors (Lo1 and Lo2) and two diodes (D3 and D4). The overall gain of the charger is improved by series charging and parallel discharging of the output inductors. A battery having a capacity of 100 Ah with a nominal voltage of 48 V is considered as a load. Furthermore, minimum sensing devices are utilized while implementing the control of the charger, which in turn reduces the control complexities and cost of the charger.

OPERATING PRINCIPLE OF CHARGER

This section describes the working principle of the charger. The symmetrical structure of the charger results in symmetrical operation during each half-cycle of supply. It is assumed that the converter operates in a steady-state condition with lossless active and passive components. Moreover, the value of Vs is considered as invariable (Vin), during a switching

 Journal Volume 10 , Iss 2, Feb 2021

cycle, due to high switching to the line frequency ratio. Despite having low-frequency ripples, it is assumed that battery current (Ibat) and voltage (Vbat) are constant in a switching cycle. Moreover, Lo1and Lo2 are assumed to have equal inductance (Lo), so

$$L_{o1} = L_{o2} = L_o$$
$$V_{Lo1} = V_{Lo2} = V_{Lo}$$
$$I_{Lo1} = I_{Lo2} = I_{Lo}. \quad (1)$$

The three operating modes during the positive half-cycle are discussed as Mode P(I)–P(III) and shown in Fig. 3.

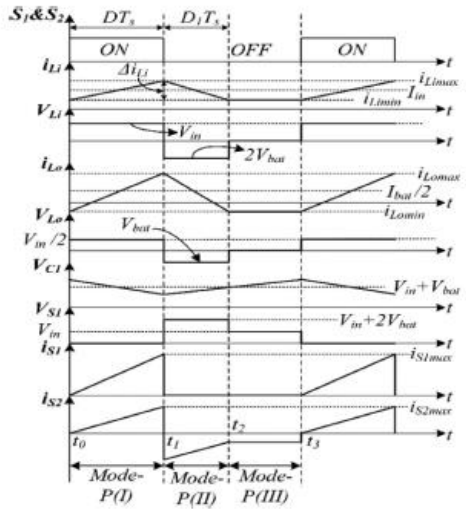

Fig. 4. Waveform of different states over a switching cycle.

A. Mode-P(I) (t0-t1)

Prior to starting of this mode, the input (iLi) and output (iLo) inductor currents have equal and opposite magnitudes, as shown in Fig. 4. Moreover, D3 and D4 are in reverse biased condition. This mode starts by turning ON switches S1 and S2 simultaneously, as shown in Fig. 3(a). The output inductors (Lo1 and Lo2) start charging by the stored energy of the intermediate capacitor C1, i.e., C1 is in discharging mode whereas Li is charged by the supply voltage. The supporting equations for this mode are as follows:

$$V_{Li} = L_i \cdot (di_{Li}/dt) = V_{in} \quad (2)$$
$$L_i = (V_{in} \cdot D \cdot T_s)/\Delta i_{Li} \quad (3)$$
$$V_{Lo1} = L_{o1}(di_{Lo1}/dt), V_{Lo2} = L_{o2}(di_{Lo2}/dt) \quad (4)$$
$$V_{Lo1} = V_{Lo2} = (V_{C1} - V_{bat})/2 \quad (5)$$
$$I_{C1} = C_1 \cdot (dv_{C1}/dt) = -I_{Lo}. \quad (6)$$

This mode ends when S1 and S2 are turned OFF

B. Mode-P(II) (t1-t2)

As the switch is turned OFF, D3 and D4 are clamped to a positive voltage and start conducting, as shown in Fig. 3(b). C1 starts charging by the input current (iLi) and the

 Journal Volume 10 , Iss 2, Feb 2021

inductor currents, i.e., iLi and iLo start decaying to zero with a negative slope, as depicted in Fig. 4. The associated mathematical expressions are shown as follows:

$$V_{Li} = V_{\text{in}} - V_{C1} - V_{\text{bat}} \quad (7)$$

$$V_{Lo1} = V_{Lo2} = -V_{\text{bat}}/2 \quad (8)$$

$$I_{C1} = I_{Li}. \quad (9)$$

This mode ends at an instant (t2) when iLi is equal and opposite of the current in output inductors, i.e., iLo. Finally, D3 and D4 stop conducting and converter enters into freewheeling mode.

C. Mode-P(III) (t2-t3)

In most cases, this mode is referred to as the freewheeling mode. The duration of this mode depends on the loading condition, switching frequency, and the value of output inductors of the converter. During this mode, both switches and diodes stop conducting, as shown in Fig. 3(c). The voltage across the Li and Lo is zero, as shown in Fig. 4:

$$V_{Li} = 0, V_{Lo} = 0 \quad (10)$$

$$I_{C1} = C_1 \cdot (dv_{C1}/dt) = I_{Li} \quad (11)$$

$$I_{Co} = C_o \cdot (dv_{\text{bat}}/dt) = -(I_{Li} + I_{\text{bat}}). \quad (12)$$

It is noteworthy that only D1 conducts for a half-cycle unlike conduction of two diodes in conventional DBR-based chargers. From (1)–(12), the dc voltage gain (M) and the average voltage across the C1 (VC1) are calculated by the volt-sec balance principle and is given by

$$V_{\text{bat}} = V_{\text{in}} \cdot D/(2 * D_1) = M \cdot V_{\text{in}} \quad (13)$$

$$V_{C1} = V_{\text{bat}} \cdot (1 + (2D_1/D)) = V_{\text{in}} + V_{\text{bat}} \quad (14)$$

where D1 represents the diodes (D5 and D6) duty ratio, as shown in Fig. 4, and M is the gain of the converter, i.e., Vbat/Vin. In a switching cycle, average current in output inductors, i.e., ILo, is half of the average battery current (Ibat), and is written as

$$I_{Lo} = I_{\text{bat}}/2 = (1/T_s)\int_0^{T_s} i_{Lo}(t) \cdot dt \quad (15)$$

$$I_{Lo} = I_{\text{bat}}/2 = [V_{\text{bat}} \cdot D_1 \cdot (D + D_1)]/(2f_s \cdot L_o) \quad (16)$$

$$I_{\text{bat}} = V_{\text{bat}}/R_L \quad (17)$$

where fs is the converter's switching frequency and RL is the fictitious load resistance. From (16) and (17), D1 is obtained as

$$D_1 = \{(L_o \cdot f_s)/[R_L \cdot (1 + 2 \cdot M)]\}^{(1/2)}. \quad (18)$$

The condition for the DCM operation is given as

$$D + D_1 < 1 \quad (19)$$

$$D_1 \cdot (1 + 2 \cdot M) < 1 \quad (20)$$

$$D_1 < 1/(1 + 2 \cdot M). \quad (21)$$

 Journal Volume 10 , Iss 2, Feb 2021

For the critical conduction case

$$D_{1\,\text{critical}} = 1/(1+2\cdot M). \qquad (22)$$

From (18) and (22), the output inductors minimum value, i.e., Locritical is calculated as

$$D_{1\text{critical}}^2 = \{(L_{\text{ocritical}}\cdot f_s)/[R_L\cdot(1+2\cdot M)]\} \qquad (23)$$

$$\frac{1}{(1+2\cdot M_{\max})^2} = \frac{L_{\text{ocritical}}\cdot f_s}{R_{L\min}\cdot(1+2\cdot M_{\max})} \qquad (24)$$

$$L_{o\text{critical}} = R_{L\min}/[f_s\cdot(1+2\cdot M_{\max})]. \qquad (25)$$

The value of Lo at the boundary of CCM and DCM operations is provided in (25). So, while selecting the output inductors, it is to be ensured that the selected value must be lower than the calculated value to implement the DCM operation of the charger over the defined range.

3. DESIGN OF CHARGER CONFIGURATION

This charger configuration is designed to operate for a broad range of Vs, i.e., from 130 V (Vsmin) to 260 V (Vsmax). The DCM mode of operation reduces the size of the output inductors. A power rating (Pmax) of 850 W is considered for the design of the charger. The variation of battery voltage (Vbat) from low SOC to full SOC is considered from 45 V (Vbatmin) to 65 V (Vbatmax), for maximizing the safety and reliability of the charger, throughout the different modes of the charging. The BSIC converter dc voltage gain is given by (13) as

$$V_{\text{bat}} = V_{\text{in}}\cdot D/(2*D_1) = M\cdot V_{\text{in}}. \qquad (26)$$

Therefore, for a complete line cycle, Vin can be written as

$$V_{\text{in}} = \sqrt{2}\cdot V_s\cdot|\sin(\omega t)|. \qquad (27)$$

By considering, input and output voltage limits, the dc voltage gain (M) varies from 0.1224 (Mmin) to 0.354 (Mmax). Moreover, by taking maximum efficiency into account, the fictitious load resistance (RL) varies from 2.38 Ω (RLmin) to 4.97 Ω (RLmax).

A.Selection of Lo1 Lo2 in DCM

The selection of output inductors is made using (25) as

$$L_{o\text{critical}} = R_{L\min}/[f_s\cdot(1+2\cdot M_{\max})]. \qquad (28)$$

The switching frequency (fs) is considered as 20 kHz. Therefore, the critical value of Lo1 and Lo2 is given as

$$L_{o\text{critical}} = 2.38/[20k\cdot(1+2\cdot 0.354)] = 69.7\,\mu\text{H}.$$

Since the selected value should be less than the calculated value, Lo1 and Lo2 having an inductance of 40 μH are selected during the implementation of the converter.

B.Selection of Li in CCM

The design of Li is carried out in CCM mode and the required value, which ensures CCM operation throughout the operation of the charger, is calculated as

 Journal Volume 10 , Iss 2, Feb 2021

$$V_{Li} = L_i \cdot (di_{Li}/dt) = V_{in} \quad (29)$$

$$L_i = (V_{in} \cdot D)/(\chi \cdot I_{Li} \cdot f_s) = (V_{in}^2 \cdot D)/(\chi \cdot I_{Li} \cdot f_s) \quad (30)$$

where Rin is the fictitious input resistance of the charger, χ is the allowable percentage current ripples, and D is the duty ratio. From (18) and (26), the range of duty ratios (D), i.e., Dmin and Dmax, is calculated as follows:

$$D_{max} = 2 \cdot M_{max} \cdot \sqrt{(L_o \cdot f_s)/(R_{L\,max} \cdot (1 + 2 \cdot M_{max}))} \quad (31)$$

$$D_{min} = 2 \cdot M_{min} \cdot \sqrt{(L_o \cdot f_s)/(R_{L\,min} \cdot (1 + 2 \cdot M_{min}))}. \quad (32)$$

From (31) and (32), Dmax and Dmin are obtained as 0.2174 and 0.1271, respectively. By considering 30% current ripple, i.e., χ = 0.30, the critical value of Li, i.e., Licritical, is given as

$$L_{icritical} = \frac{V_{inmax}^2 \cdot D_{max}}{P_{max} \cdot \chi \cdot f_s} = \frac{(\sqrt{2} \cdot V_{smax}) \cdot D_{max}}{P_{max} \cdot \chi \cdot f_s} \quad (33)$$

$$L_{icritical} = \frac{(\sqrt{2} \cdot 260)^2 \cdot 0.2174}{850 \cdot 0.3 \cdot 20 \cdot 10^3} = 5.76\,mH.$$

Therefore, to ensure CCM operation, Li is selected as 6 mH.

C. Selection of C1 in CCM

The selection of C1 is critical because of two different restrictions on the capacitor voltage profile. In a switching cycle, the voltage across C1 should be constant, whereas, in a complete line cycle, the voltage should follow the supply voltage profile. Therefore, the value of C1 is calculated as

$$C_1 = 1/\{\omega_{res}^2 \cdot (L_i + L_{o1} + L_{o2})\}. \quad (34)$$

where ωres defines the frequency of resonance between C1, Li, Lo1, and Lo2. The selected ωres should be high enough to the line frequency but lower than the switching frequency:

$$C_1 = 1/\{(2 \cdot \pi \cdot 2000)^2 \cdot (6m + 2 \cdot 40\mu)\} = 1.1\,\mu F.$$

The selected value of C1 is 0.94 μF.

D.Selection of CDC

CDC is designed to minimize the flow of low-frequency ripple power into the battery, during charging without exceeding defined voltage ripple limit (λ) [22]. The size of CDC is mainly decided by the power and voltage handling limit set as per application requirement. CDC is calculated as

$$C_{DC} = P_{max}/(4\pi \cdot f_{Line} \cdot \lambda \cdot V_{batmax}^2) \quad (35)$$

where fline is the supply frequency. Considering 3% ripple, CDC is calculated as

Research paper **© 2012 IJFANS. All Rights Reserved, Journal Volume 10 , Iss 2, Feb 2021**

$$C_{DC} = 850/\left(4\pi \cdot 50 \cdot 0.03 \cdot (65)^2\right) = 10.66\,\text{mF}.$$

Therefore, C_{DC} is taken as 11.75 mF.

CONTROL TECHNIQUE

The BSIC converter is controlled to achieve two main objectives by incorporating minimum cost and complexities during the implementation. The prime objective of the controller is to control the charging current to the battery in CC and CV modes, as per the requirement. In addition to that, low distortion in supply current along with unity power factor operation at the supply side is another important objective of the control. The overall control is implemented by a conventional dual loop structure, as given in Fig. 2, using Texas Instruments (TI) TMS320F28377S DSP. The outer loop is employed to tackle the variations in Vbat whereas the inner loop takes care of Ibat while maintaining the UPF operation with minimum supply current distortions. For the outer loop, Vbat is sensed by utilizing a voltage sensor, and the switching frequency ripples are filtered out from it by employing a low-pass filter (LPF). In order to get the reference battery current (Ibat∗), the filtered Vbat is matched with Vbat, i.e., Vbat∗, and the error (Vbate) is fed to a voltage proportional-integral (PI) controller. The output of voltage PI controller provides the required Ibat∗. The expressions for outer loop are given as

$$V_{\text{bate}}(k) = V^*_{\text{bat}}(k) - V_{\text{bat}}(k) \tag{36}$$

$$I^*_{\text{bat}}(k) = I^*_{\text{bat}}(k-1) + k_{pV}\{V_{\text{bate}}(k) - V_{\text{bate}}(k-1)\} + k_{iV} \cdot V_{\text{bate}}(k) \tag{37}$$

where kpV is the proportional gain, kiV is the integral gain of the voltage PI controller, and k is the kth sampling instant. For implementing inner loop control, the charging current Ibat is sensed through a current sensor and filtered by an LPF. The filtered current is then compared with Ibat∗ and the error (Ie) is passed through the current PI controller. The output of the PI controller provides the required duty ratio (mc) as

$$I_e(k) = I^*_{\text{bat}}(k) - I_{\text{bat}}(k) \tag{38}$$

$$m^*_c(k) = m^*_c(k-1) + k_{pI}\{I_e(k) - I_e(k-1)\} + k_{iI} \cdot I_e(k) \tag{39}$$

where kpI and kiI are, respectively, the proportional and integral constants of the current PI controller. The duty ratio (mc) is then compared with a sawtooth carrier waveform. The comparison provides the required gate drive signals for switches (S1 and S2). It is noteworthy that the switching signal is applied to S1 and S2, simultaneously, to reduce the complexity of the control.

Pulse width Modulation

Pulse Width Modulation (PWM) is the most effective means to achieve constant voltage battery charging by switching the solar system controller's power devices. When in PWM regulation, the current from the solar array tapers according to the battery's condition and recharging needs consider a waveform such as this: it is a voltage switching between 0v and 12v. It is fairly obvious that, since the voltage is at 12v for exactly as long as it is at 0v, then a 'suitable device' connected to its output will see the average voltage and think it is being fed

 Journal Volume 10 , Iss 2, Feb 2021

6v - exactly half of 12v. So by varying the width of the positive pulse - we can vary the 'average' voltage.

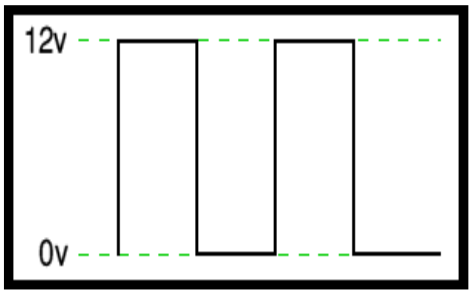

Fig.4.1 Average voltage exactly half of 12v

Similarly, if the switches keep the voltage at 12 for 3 times as long as at 0v, the average will be 3/4 of 12v - or 9v, as shown below.

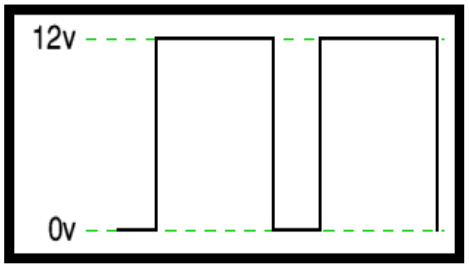

Fig.4.2 Average voltage will be 3/4 of 12v

and if the output pulse of 12v lasts only 25% of the overall time, then the average is

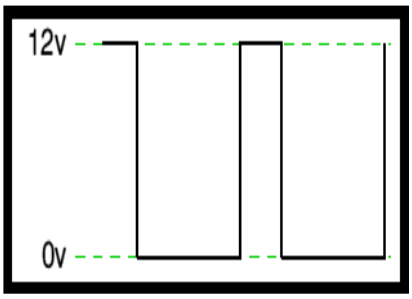

Fig.4.3Average output voltage at 12v

By varying - or 'modulating' - the time that the output is at 12v (i.e. the width of the positive pulse) we can alter the average voltage. So we are doing 'pulse width modulation'. I said earlier that the output had to feed 'a suitable device'. A radio would not work from this: the radio would see 12v then 0v, and would probably not work properly. However a device such as a motor will respond to the average, so PWM is a natural for motor control.

PI CONTROLLER

A variation of Proportional Integral Derivative (PID) control is to use only the proportional and integral terms as PI control. The PI controller is the most popular variation, even more than full PID controllers. The value of the controller output u(t) is fed into the system as the manipulated variable input.

$e(t)=SP-PV$

$u(t)=ubias+Kce(t)+\frac{Kc}{\tau I}\int_0^t e(t)dt$

Research paper **© 2012 IJFANS. All Rights Reserved, Journal Volume 10 , Iss 2, Feb 2021**

The ubias term is a constant that is typically set to the value of u(t) when the controller is first switched from manual to automatic mode. This gives "bumpless" transfer if the error is zero when the controller is turned on. The two tuning values for a PI controller are the controller gain, Kc and the integral time constant τI. The value of Kc is a multiplier on the proportional error and integral term and a higher value makes the controller more aggressive at responding to errors away from the set point. The set point (*SP*) is the target value and process variable (*PV*) is the measured value that may deviate from the desired value. The error from the set point is the difference between the *SP* and *PV* and is defined as e(t)=SP−PV

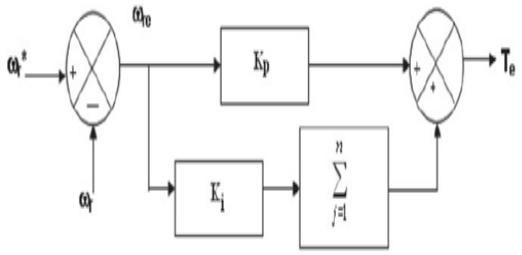

Fig.5.1.Block diagram of PI speed controller

4. RESULTS

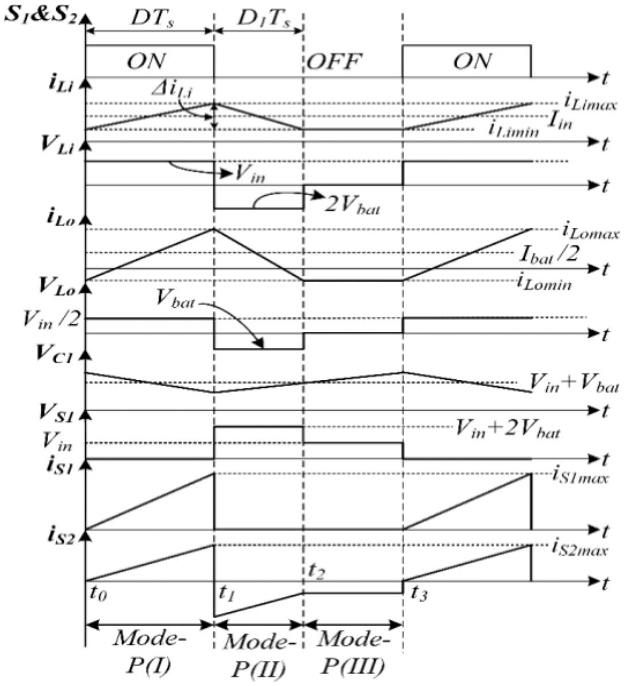

Fig: Simulation Waveforms

Research paper **© 2012 IJFANS. All Rights Reserved, Journal Volume 10 , Iss 2, Feb 2021**

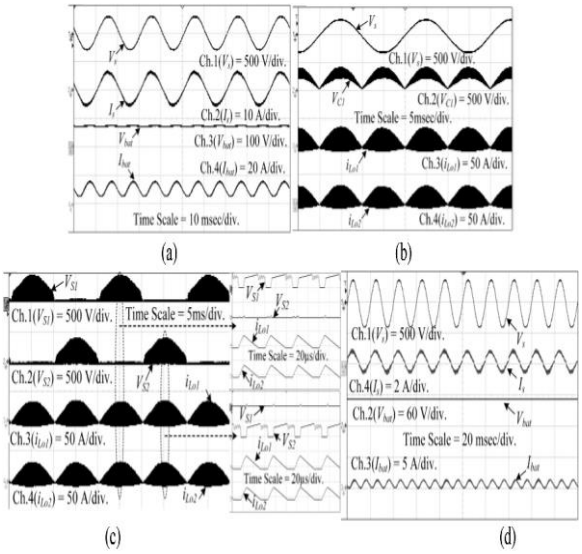

Fig: Generated OutputWaveforms

5. CONCLUSION

In this article, a bridgeless switched inductor Cuk (BSIC) PFC converter based charger has been put forward, to provide a single-phase single-stage transformerless charging solution for the LEVs. This charger has alleviated the drawback of limited step-down dc voltage gain in conventional dc–dc converters. Therefore, the higher step-down voltage gain has been availed for the LEVs batteries, without employing a transformer. The CC and CV modes have been accomplished in a single-stage with excellent supply-side power quality indices such as power factor, distortion factor, and supply current THD. Furthermore, fewer sensing devices with optimized control complexities have been considered while implementing the control of the charger. Moreover, the design of the charger has been carried out in a way to enhance the safety and reliability of its components while operating over the defined supply voltage and battery voltage range. The test results under the steady-state and during various dynamics have been demonstrated to support the theoretical analysis. The operation of the charger during line and load regulation has been tested and verified. A short comparison of the presented BSIC converter based charger with the other charger topologies has been carried out and presented in a tabular form. Finally, it has been shown that the presented charger configuration is advantageous in many ways such as low cost, less size, enhanced supply-side performances, minimum components counts, and fewer control complexities.

6. REFERENCES

1. NITI Aayog and WEC, "Zero-emission vehicles: Towards a policy framework," NITI Aayog, New Delhi, India, Rep., 2008. [Onlne]. Available:https://niti.gov.in/writereaddata/files/document_publication/ EV_report.pdf
2. Z. Yang and P. C. Sen, “Recent developments in high power factor switch-mode converters,” in Proc. IEEE Can. Conf. Electron. Comp. Eng., Waterloo, ON, Canada, 1998, vol. 2, pp. 477–480.
3. H. Wang, S. Dusmez, and A. Khaligh, “A novel approach to design EV battery chargers using SEPIC PFC stage and optimal operating point tracking technique for LLC converter,” in Proc. IEEE App. Power Electron. Conf. Expo., Fort Worth, TX, USA, 2014, pp. 1683–1689.

4. R. Pandey and B. Singh, "A power-factor-corrected LLC resonant converter for electric vehicle charger using Cuk converter," IEEE Trans. Indus. Appl., vol. 55, no. 6, pp. 6278–6286, Nov–Dec. 2019.
5. D. Kim and B. Lee, "Asymmetric control algorithm for increasing efficiency of nonisolated on-board battery chargers with a single controller," IEEE Trans. Veh. Technol., vol. 66, no. 8, pp. 6693–6706, Aug. 2017.
6. A. V. J. S. Praneeth and S. S. Williamson, "A wide input and output voltage range battery charger using buck-boost power factor correction converter," in Proc. IEEE Appl. Power Electron. Conf. Expo., Anaheim, CA, USA, 2019, pp. 2974–2979.
7. S. Ryu, D. Kim, M. Kim, J. Kim, and B. Lee, "Adjustable frequency–dutycycle hybrid control strategy for full-bridge series resonant converters in electric vehicle chargers," IEEE Trans. Indus. Electron., vol. 61, no. 10, pp. 5354–5362, Oct. 2014.